Design of a Mechanical Tunable Resonant Fast Steering Mirror

Johannes Schlarp, Ernst Csencsics, Gabriel Doblinger and Georg Schitter

***Abstract*— This work present the design, simulation and control of a mechanical tunable resonant fast steering mirror (FSM). The proposed system design enables to tune each of the two hybrid reluctance actuated system axis individually, such that the power consumption can be improved. By adapting the effective length of the flexure with clamps, the stiffness of each system axis can be adjusted. The position of the clamps is varied with stepper motors, such that the resonance frequency can be tuned between 138 Hz and 263 Hz. A tuning algorithm automatically adapts the position of the clamps according to the selected scan trajectory, such that the FSM is operated with maximum efficiency. Experimental results show, that the power consumption can be enhanced through the mechanical tuning of the resonance frequency by a factor of 13.83 as compared to a conventional FSM.**

I. Introduction

Fast steering mirrors (FSMs) are compact opto-mechatronic tip/tilt systems, which are employed in various optical applications, such as free-space optical communication [1], material processing [2], beam stabilization [3], target tracking [4] or optical three dimensional (3D) measurement systems [5]. FSMs are typically controlled by a feedback motion controller, such that a high bandwidth and good disturbance rejection is achieved [6]. They are driven by electromagnetic [2], [7] or piezoelectric actuators [8], such that either a large actuation range or a high bandwidth is achieved. Recently, hybrid reluctance actuation (HRA) has been employed for the rotational motion of the FSM [9]. This actuation principle uses a permanent magnet to generate a constant biasing flux. With a steering flux, which is generated by coils, the position of the mover can be changed. The mover is suspended by a flexure, such that the non-actuated DoF are restricted and the negative stiffens caused by the permanent magnet is compensated. Compared to voice coil actuators a higher motor constant can be achieved, which reduces the overall power consumption and thus the thermal stress caused by heated coils [10].

Optical scanning three dimensional measurement systems, e.g. scanning triangulation sensor system, require a large actuation range, such that electromagnetic actuators are typically used [11]. To scan the area of interest on the sample, raster or Lissajous-based scan trajectories are commonly employed [12]. The amplitude and frequency of the scan trajectory are typically kept constant during a scan. However, if the area of interest on the sample changes, the scan trajectories are adjusted accordingly [13]. The achievable resolution of the scanning system is partially limited by the heat dissipated from the FSM [14]. The achievable bandwidth for large scan amplitudes is, however, limited by the maximum applicable current through the coils, such that a trade-off between resolution and bandwidth has to be made [10]. Nevertheless, the system should be operated with maximum efficiency.

One system axis from the FSM can be modelled by a mass-spring-damper system [10]. The system features a resonance frequency at which the gain is much higher compared to all other frequencies. This is caused by the fact, that the applied force is in phase with the velocity, such that the actuator force is transformed in mechanical movement with maximum efficiency [15]. In [16] the resonance frequencies of both system axes are tuned to match the drive frequencies of the Lissajous-based scan trajectory. This leads to an improved energy efficiency by a factor of 100. However, the selected scan amplitude and frequency can not be changed, since the system is tuned for one specific scan trajectory.

The contribution of this paper is the system design and validation of a mechanical tunable resonant fast steering mirror, which adapts the stiffness of the flexure by clamps, to reduce the overall power consumption. Section II presents the design of the mechanical tuning structure and the integration in the FSM. In Section III the achievable tuning range is determined using FEM simulations. The experimental setup, system hardware and control structure is presented in Section IV, while the tuning algorithm is further described in Section V. The measurement results are shown and validated in Section VI. Finally, Section VII concludes the paper.

II. System Design

The cross sectional view of the proposed tunable hybrid reluctance actuated FSM is depicted in Fig. 1. The main components of the FSM are a cylindrical permanent magnet, ferromagnetic mover and yoke, flexure, pivot bearing, four coils and position sensors. The two system axes are arranged perpendicular to each other, such that the yoke is cross shaped. The magnet in the center of the FSM generates a biasing flux in the mover, yoke and air gap between them. For each system axis two coils are connected in series with opposite current directions. If a current is applied to the coils, a magnetic flux is generated which passes through the yoke, mover and two air gaps. The flux from the coils and from the magnet are superimposed, such that a current through the coils leads to an increased flux in one air gap and a decreased flux in the opposite one, which results in a torque on the mover. The pivot bearing is designed to suspend the mover

The authors are with the Christian Doppler Laboratory for Precision Engineering for Automated In-Line Metrology at the Automation and Control Institute (ACIN), Technische Universität Wien, 1040 Vienna, Austria. Corresponding author: schlarp@acin.tuwien.ac.at

Post-print version of the article: J. Schlarp, E. Csencsics, G. Doblinger and G. Schitter, "Design of a Mechanical Tunable Resonant Fast Steering Mirror", *IEEE/ASME International Conference on Advanced Intelligent Mechatronics (AIM)*, pp. 1607–1612, 2020. DOI: 10.1109/AIM43001.2020.9159032

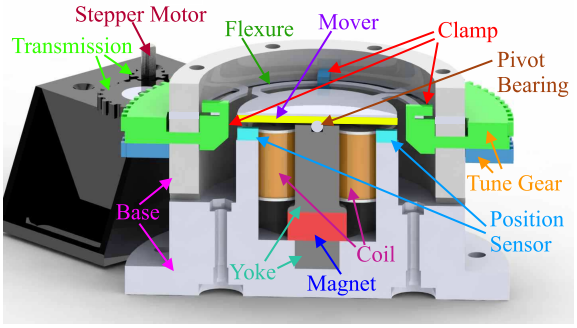

Fig. 1. Concept of the mechanical tunable FSM. The effective arm length of the flexure can be changed by clamps. For each system axis two clamps are used and bonded to the same tune gear. The angular position of each tune gear is varied by a stepper motor.

and to fix the point of rotation. The four position sensors beneath the mover measure the angular positions Θ of both system axes. To compensate the negative stiffness induced by the permanent magnet, a flexure is used [10]. The flexure composes out of four flexure arms, which connect the base of the FSM with the mover. Figure 2 shows the shape of the flexure. The flexure is aligned, such that only the two opposing flexure arms deform, if one system axis is actuated.

The resonance frequency ω_r of each system axis is defined by the rotational stiffness k and the moment of inertia J in the following form

$$\omega_r = \sqrt{\frac{k}{J}}. \tag{1}$$

The resonance frequency can be tuned towards higher frequencies by either reducing the moment of inertia, or increasing the stiffness. The moment of inertia can, however, not be further reduced, since it is fixed by the mover geometry and material density. The rotational stiffness of each system axis is defined by the width, thickness and arm length of two opposing flexure arms. By shortening the effective flexure arm length the stiffness and subsequently the resonance frequency is increased. This is realized using clamps, which restrict a movement of the flexure between the base and the clamps. By changing the angular position of the clamps, the resonance frequency can be varied. To change the position of the two opposing clamps equally, they are bonded to one tune gear, which is guided by the base. The clamps can be actuated from the outside through cut outs in the base. Since both system axes should be tuned individually, two tune gears and four clamps are used. Figure 2 shows the design of the clamps and tune gears. As can be observed, the angular clamp position φ can be changed between 30.5° and 59.5°. The position of each tune gear and thus the clamp positions can be changed with a stepper motor. In order to increase the torque on the tune gear, a transmission is used, which is shown in Fig. 1. The effective gear diameters are 12.26 mm, 31.58 mm and 130.73 mm for the motor gear, intermediate gear and tune gear, respectively. The resulting

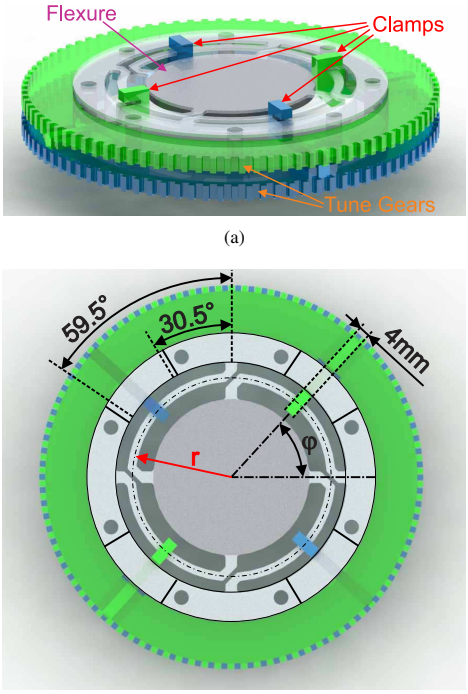

Fig. 2. (a) CAD rendering of the tuning mechanism. The flexure consists out of four flexure arms. Two opposing arms define the stiffness of one system axis. Due to the perpendicular setup, the resonance frequency of each axis can be tuned independently. (b) The effective arm length is variable between 30.5° and 59.5°, using the clamps.

transmission ratio between the tune gear and stepper motor is 1:10.7.

III. Simulation

To calculate the achievable tuning range up front, a FEM simulation (Type: Ansys, Ansys Inc., USA) is performed. For simplicity, only the flexure, mover and clamps are employed in the simulation. The effects regarding the hybrid reluctance actuation principle, are not considered, but further described in [10]. The material of the mover is steel (EN 10025 S 235 JR), while the flexure is made out of aluminium (AW 1050). The base, clamps and gears are 3D-printed (Type: Prusa I3 MK3S, Prusa Research, Czech Republic) out of plastic (PET). To determine the resonance frequency, a modal analysis is performed for various clamp positions. Figure 3 shows the derived frequency responses. The damping ratio and rotational inertia are obtained from prior measurements (see [10]). As can be observed, the resonance frequency is tunable between 176.7 Hz and 383.1 Hz.

An analytic model for the stiffness k of the flexure, can be given by

$$k = 2Ewt^3/l^3, \tag{2}$$

with E the Young's modulus, t the thickness, w the width and l the effective arm length of the flexure [17]. As can be

Post-print version of the article: J. Schlarp, E. Csencsics, G. Doblinger and G. Schitter, "Design of a Mechanical Tunable Resonant Fast Steering Mirror", *IEEE/ASME International Conference on Advanced Intelligent Mechatronics (AIM)*, pp. 1607–1612, 2020. DOI: 10.1109/AIM43001.2020.9159032

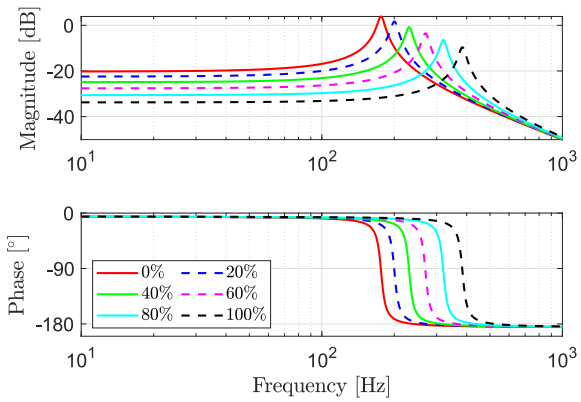

Fig. 3. Simulated frequency response for different clamp positions φ between 0 % (30.5°) and 100 % (59.5°). The simulateds tuning range is between 176.7 Hz and 383.1 Hz.

observed, the stiffness increases with the power of three, for a decreasing flexure length. The effective flexure arm length l can be calculated with respect to the angular clamp position φ in the following form

$$l = 2r\left(\frac{\pi}{2} - \varphi\right), \tag{3}$$

with r the effective radius of the flexure (see Fig. 2). By rearranging (1), (2) and (3), the influence of the angular clamp position on the resonance frequency can be given by

$$\omega_r = \sqrt{\frac{Ewt^3}{4Jr^3\left(\frac{\pi}{2} - \varphi\right)^3}}\,. \tag{4}$$

IV. System Hardware

Figure 4 depicts the experimental setup of the mechanical tunable resonant fast steering mirror. The angular positions

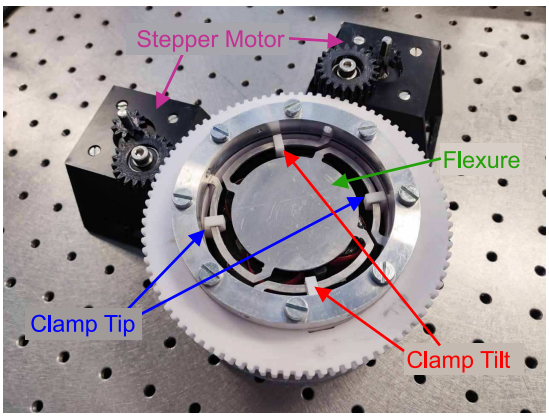

Fig. 4. Experimental setup of the mechanical tunable FSM. The angular position of the clamps can be varied with a stepper motor for each system axis. The clamps, tuning gears and holders for the stepper motor are 3D-printed.

of the two tune gears are changed by stepper motors (Type: 42SH38-4A, RS Components, United Kingdom). The step angle of the motors are 1.8°. As already described in Section II the gear ratio is 1:10.7, such that one step of the motor corresponds to 0.1688°. The stepper motors are controlled by stepper drivers (Type: DRV8825, Texas Instruments, USA), which are operated in the full step mode.

Figure 5 depicts the applied control structure for each system axis. A rapid prototyping platform (Type: DS1202, dSPACE GmbH, Germany) is used to control the angular positions of the FSM Θ and to tune the resonance frequencies. The current controllers are implemented on the FPGA of the rapid prototyping platform, with a bandwidth of 30 kHz. Two custom made current amplifiers (Type: MP38CL, Apex Microtechnology, USA) are used to drive the system axes of the FSM. The bandwidth of the position control is much lower (∼1 kHz) as compared to the internal current loop, such that for the design of the position controller, the current loop can be assumed as a direct feed-through. The measured current serves as the input for the tuning algorithm, which calculates the required steps and movement direction of the stepper motor.

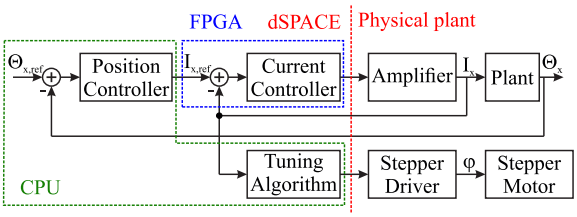

Fig. 5. Control structure applied to each system axis of the FSM. The inner loop consists out of a current controller. The angular position Θ_x of the FSM is controlled in the outer loop. The measured current I_x serves as an input for the tuning algorithm, which manipulates the position of the tune gear via a stepper driver and motor.

To determine the system dynamics for various clamp positions φ, a system analyzer (Type: 3562A, Hewlett-Packard, USA) is used. The current through the coil I and the calculated angular position Θ serve as system input and output, respectively. Figure 6 shows the the measured system dynamics for various clamp positions. As can be observed, the resonance frequency is tunable between 138 Hz and 263 Hz. At the resonance frequencies a large gain peaking (>18 dB) is observable, which enables an improved power consumption. Compared to the simulation, the achievable tuning range (176.7 Hz and 383.1 Hz) is by a factor of 1.65 smaller and shifted towards lower frequencies. In the simulation only the behaviour of the flexure, mover and clamps has been simulated (see Section III). Furthermore, lateral movements of the clamps were restricted by boundary conditions, which encourage the measured lower resonance frequencies. The shift and smaller tuning range is most probably caused by the limited stiffness of the base (3D-printed) and manufacturing tolerances [18], which were not considered in the simulation. In the measured phase an additional phase-lag is observable, which is caused by eddy currents

Post-print version of the article: J. Schlarp, E. Csencsics, G. Doblinger and G. Schitter, "Design of a Mechanical Tunable Resonant Fast Steering Mirror", *IEEE/ASME International Conference on Advanced Intelligent Mechatronics (AIM)*, pp. 1607–1612, 2020. DOI: 10.1109/AIM43001.2020.9159032

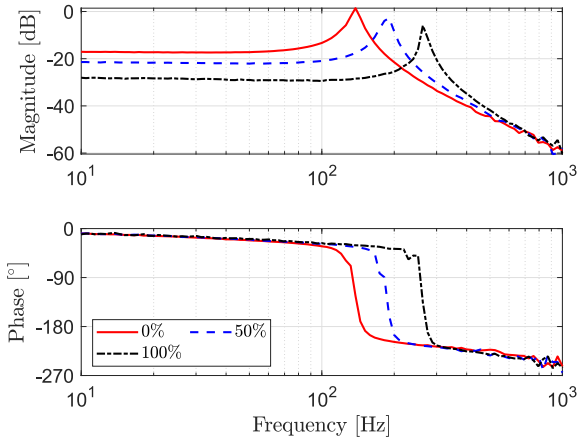

Fig. 6. Measured frequency response for different clamp positions. The resonance frequency can be varied between 138 Hz and 263 Hz. The gain at the resonance frequency is at least 18 dB higher as compared to the DC gain.

in the actuator [10], the bandwidth of the position sensor system (10 kHz) and the time delay of the dSpace platform (40 kHz).

V. Tuning Algorithm

Figure 7 depicts the flow chart of the tuning algorithm for one system axis.

Step 1: The selected scan trajectory is applied to both system axes of the FSM. The feedback controllers ensure that each system axis follows the scan trajectory, even though the resonance frequency is changed.

Step 2: The clamps are moved to the position φ with the highest resonance frequency, which is at 59.5°. This position serves as the reference.

Step 3: At this position the root mean squared (rms) current is measured, since it corresponds to the overall power consumption.

Step 4: The angular clamp position φ is decreased by one step (0.1688°).

Step 5: The rms current is measured at the present clamp position.

Step 6: The measured current is compared to the one from the previous step. If the rms current is almost equal (noise) or smaller, the optimum has yet not been found, such that step 7 is performed. Otherwise step 8 is processed.

Step 7: If the minimum clamp position (30.5°) is reached, the tuning algorithm is stopped, since this position requires the least amount of energy. Otherwise the clamp position is further reduced in step 4.

Step 8: The position, which requires the least amount of energy was obtained at the previous clamp position, such that the current position is increased by one step.

The cycling time at each iteration is roughly around one second and strongly depends on the selected scan frequency,

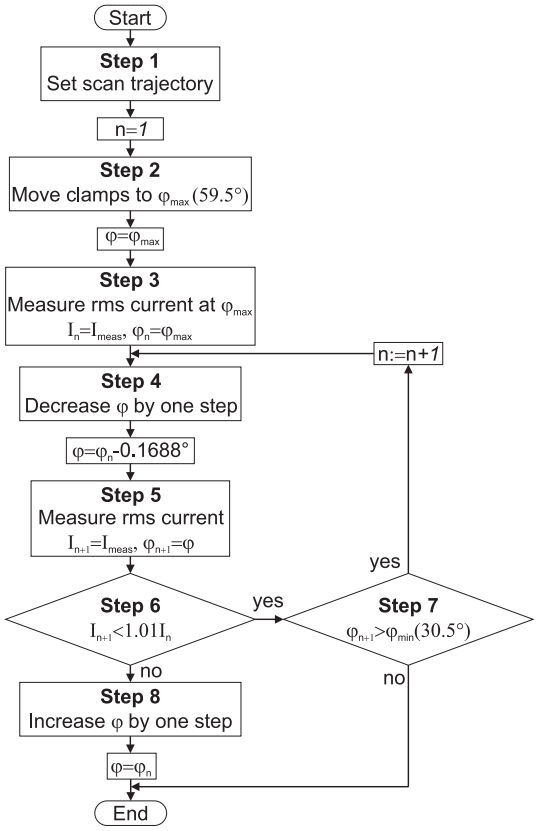

Fig. 7. Flowchart of the tuning algorithm for one system axis. The algorithm minimizes the current consumption of the FSM by varying the clamp position.

since the rms current is measured over ten periods of the selected frequency. Furthermore, the cycling time also depends on the selected amplitude, since the measurement is started when transients have decayed.

The position controller is required to ensure that the system axis precisely follow the scan trajectory, even though the resonance frequency is changed. As can be observed in Fig. 6, the mass line of the system is constant, since only the stiffness of the system is changed (see Section II). If the crossover frequency of the open loop system is located on the mass line, the resonance frequency can be tuned without impairing the motion control. A PID controller is used for the position control of the FSM (see Fig. 5). The crossover frequency is selected to 700 Hz and the controller parameters are obtained with the PID alpha tuning method ($\alpha = 3$), which is further described in [19]. Figure 8 shows the frequency response of the PID controller and the open loop system for various clamp positions. As can be observed, the crossover frequency (700 Hz) is equal for the different clamp positions and the phase margin (PM) of the system is 22°.

Post-print version of the article: J. Schlarp, E. Csencsics, G. Doblinger and G. Schitter, "Design of a Mechanical Tunable Resonant Fast Steering Mirror", *IEEE/ASME International Conference on Advanced Intelligent Mechatronics (AIM)*, pp. 1607–1612, 2020. DOI: 10.1109/AIM43001.2020.9159032

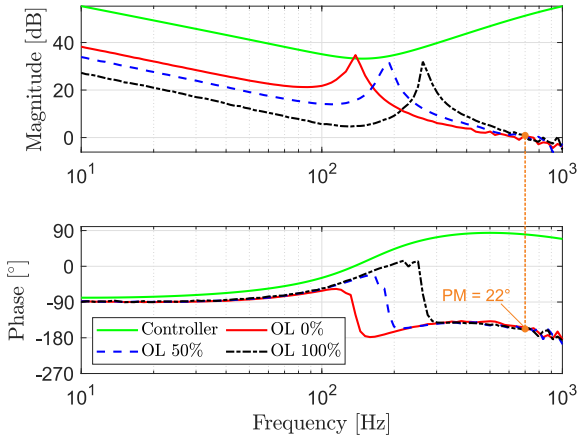

Fig. 8. Open loop frequency response of one system axis for various clamp positions, and the frequency response of the controller (green). The open loop crossover frequency is for all clamp position 700 Hz and well above the resonance frequencies.

VI. Experimental results

To evaluate the system performance a sinusoidal angular position signal Θ, with a frequency of 130 Hz, is applied to one system axis of the FSM and the current consumption is measured at various scan amplitudes. The results of the tuned FSM are compared to a conventional FSM, which is realized by moving the clamps to the minimum clamp position ($\varphi = 30.5°$). Figure 9(a) shows the measured current amplitude for different scan amplitudes. The current amplitude of the conventional and tuned FSM are identical for small scan amplitudes, since the minimum angular position requires the least amount of energy. According to Fig. 6 the minimum stiffness should lead to the lowest power consumption at every amplitude. However, the negative stiffness of the actuator increases towards larger scan amplitudes (see [10]), such that the resonance frequency is shifted towards lower values. Measurements of the conventional FSM are stopped at 0.56°, since the maximum current amplitude of 3 A is reached. The current increases only gradually towards larger scan amplitudes, due to the tuning algorithm. The unsteady slope is caused by the finite step resolution of the stepper motors (0.1688°), such that the resonance frequency can not be perfectly matched to the driving frequency. The current amplitude at 0.56° is 0.815 A for the tuned system, which is by a factor of 3.681 lower as compared to the conventional FSM.

The measured rms current is shown in Fig. 9(b) and used to calculate the power consumption of the FSM. Therefore, the current amplitude can not be used, since the current through the coils does not necessarily have to be sinusoidal. The curve shapes of both system are similar to the one of the current amplitudes. A current consumption of 0.8 A is observable at 0.35° for the conventional system and 0.89° for the tuned system, such that a by factor of 2.54 larger scan

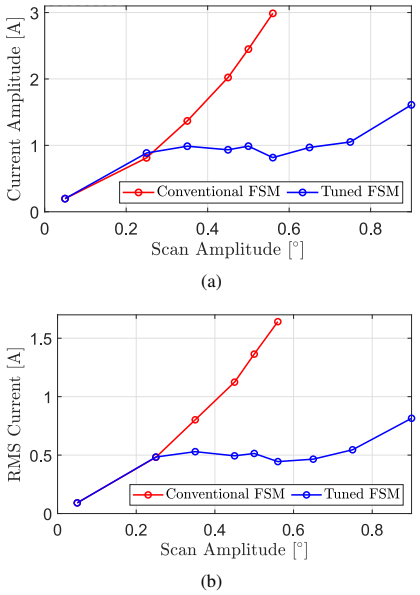

Fig. 9. Comparison of the current consumption of the conventional (red) and tuned (blue) FSM system for different scan amplitudes. (a) compares the current amplitude. The conventional system reaches the maximum current of 3 A at 0.56°. (b) shows the root mean squared current for both systems.

range is achieved. At a scan amplitude of 0.56° the measured current I_{rms} is 1.64 A and 0.44 A for the conventional and tuned system, respectively. The power consumption P is calculated, as follows

$$P = I_{rms}^2 R, \tag{5}$$

with the coil resistance R of 5.3 Ω. The resulting power consumption at a scan amplitude of 0.56° is 14.25 W for the conventional and 1.03 W for the tuned system. Through the tuning process the power consumption is decreased by a factor of 13.83 as compared to a conventional FSM.

In summary the design, algorithm and validation of a mechanical tunable hybrid reluctance actuated FSM is shown, enabling to tune the resonance frequency between 138 Hz and 263 Hz and improve the power consumption by a factor of 13.83 as compared to a conventional FSM.

VII. Conclusion

In this paper the design, tuning algorithm and validation of a mechanical tunable resonant FSM are shown. The stiffness of each system axis of the hybrid reluctance actuated FSM can be individually tuned by clamps, which adapt the effective arm length of the flexure. The angular position of the clamps can be changed by stepper motors between 30.5° and 59.5°. Simulations are performed to calculate the achievable tuning range up front. Measurement results show that the resonance frequency can be tuned between 138 Hz and 263 Hz. The tuning algorithm automatically adapts the clamp position, such that the FSM is operated with maximum

Post-print version of the article: J. Schlarp, E. Csencsics, G. Doblinger and G. Schitter, "Design of a Mechanical Tunable Resonant Fast Steering Mirror", *IEEE/ASME International Conference on Advanced Intelligent Mechatronics (AIM)*, pp. 1607–1612, 2020. DOI: 10.1109/AIM43001.2020.9159032

efficiency. Experimental results show, that the scan range of the tuned system is by a factor of 2.54 larger, as compared to a conventional FSM. Furthermore, the power consumption at a fixed scan amplitude is improved by a factor 13.83 through the tuning of the resonance frequency.

ACKNOWLEDGMENT

The financial support by the Austrian Federal Ministry for Digital, Business and Enterprise, and the National Foundation for Research, Technology and Development, as well as MICRO-EPSILON MESSTECHNIK GmbH & Co. KG and ATENSOR Engineering and Technology Systems is gratefully acknowledged.

REFERENCES

[1] A. Sinn, T. Riel, F. Deisl, S. Schachner, and G. Schitter, "High-bandwidth tip-tilt vibration compensation in telescope systems," *IFAC-PapersOnLine*, vol. 52, no. 15, pp. 549–554, 2019.

[2] M. Hafez, T. Sidler, R. Salathe, G. Jansen, and J. Compter, "Design, simulations and experimental investigations of a compact single mirror tip/tilt laser scanner," *Mechatronics*, vol. 10, no. 7, pp. 741–760, 2000.

[3] L. R. Hedding, "Fast steering mirror design and performance for stabilization and single axis scanning," in *Acquisition, Tracking, and Pointing IV*, vol. 1304. International Society for Optics and Photonics, 1990, p. 14.

[4] R. W. Cochran and R. H. Vassar, "Fast-steering mirrors in optical control systems," in *Advances in Optical Structure Systems*, vol. 1303. International Society for Optics and Photonics, 1990, pp. 245–251.

[5] J. Schlarp, E. Csencsics, and G. Schitter, "Optical scanning of a laser triangulation sensor for 3d imaging," *IEEE Transactions on Instrumentation and Measurement*, 2019, accepted.

[6] Y.-X. Xia, Q.-L. Bao, and Q.-Y. Wu, "Internal model control of a fast steering mirror for electro-optical fine tracking," in *High-Power Lasers and Applications V*, vol. 7843. International Society for Optics and Photonics, 2010, p. 78430L.

[7] E. Csencsics, J. Schlarp, T. Schopf, and G. Schitter, "Compact high performance hybrid reluctance actuated fast steering mirror system," *Mechatronics*, vol. 62, 2019.

[8] J.-H. Park, H.-S. Lee, J.-H. Lee, S.-N. Yun, Y.-B. Ham, and D.-W. Yun, "Design of a piezoelectric-driven tilt mirror for a fast laser scanner," *Japanese Journal of Applied Physics*, vol. 51, no. 9S2, p. 09MD14, 2012.

[9] D. J. Kluk, M. T. Boulet, and D. L. Trumper, "A high-bandwidth, high-precision, two-axis steering mirror with moving iron actuator," *Mechatronics*, vol. 22, no. 3, pp. 257–270, 2012.

[10] E. Csencsics, J. Schlarp, and G. Schitter, "High performance hybrid-reluctance-force-based tip/tilt system: Design, control and evaluation," *IEEE Transactions on Mechatronics*, vol. 23, no. 5, pp. 2494–2502, 2018.

[11] J. Schlarp, E. Csencsics, and G. Schitter, "Scanning laser triangulation sensor geometry maintaining imaging condition," *IFAC-PapersOnLine*, vol. 52, no. 15, pp. 301–306, 2019.

[12] T. Tuma, J. Lygeros, A. Sebastian, and A. Pantazi, "Optimal scan trajectories for high-speed scanning probe microscopy," in *American Control Conference (ACC), 2012*. IEEE, 2012, pp. 3791–3796.

[13] J. Schlarp, E. Csencsics, and G. Schitter, "Feature detection and scan area selection for 3d laser scanning sensors," in *2018 IEEE/ASME International Conference on Advanced Intelligent Mechatronics (AIM)*. IEEE, 2018, pp. 280–285.

[14] T. H. Jamieson, "Thermal effects in optical systems," *Optical Engineering*, vol. 20, no. 2, p. 202156, 1981.

[15] R. M. Schmidt, G. Schitter, and A. Rankers, *The Design of High Performance Mechatronics*. IOS Press, 2014.

[16] E. Csencsics and G. Schitter, "System design and control of a resonant fast steering mirror for lissajous-based scanning," *IEEE Transactions on Mechatronics*, vol. 22, no. 5, pp. 1963–1972, 2017.

[17] S. Ito, F. Cigarini, S. Unger, and G. Schitter, "Flexure design for precision positioning using low-stiffness actuators," *IFAC-PapersOnLine*, vol. 49, no. 21, pp. 200–205, 2016.

[18] B. Tymrak, M. Kreiger, and J. M. Pearce, "Mechanical properties of components fabricated with open-source 3-d printers under realistic environmental conditions," *Materials & Design*, vol. 58, pp. 242–246, 2014.

[19] E. Csencsics and G. Schitter, "Parametric PID controller tuning for a fast steering mirror," in *1st IEEE Conference on Control Technology and Applications*, Kohala Coast, Hawaii, USA, 2017.

Post-print version of the article: J. Schlarp, E. Csencsics, G. Doblinger and G. Schitter, "Design of a Mechanical Tunable Resonant Fast Steering Mirror", *IEEE/ASME International Conference on Advanced Intelligent Mechatronics (AIM)*, pp. 1607–1612, 2020. DOI: 10.1109/AIM43001.2020.9159032